Clinical Anatomy 32:914–928 (2019)

ORIGINAL COMMUNICATION

Suboccipital Myodural Bridges Revisited:
Application to Cervicogenic Headaches

KEI KITAMURA,[1] KWANG HO CHO,[2]* MASAHITO YAMAMOTO,[3] MICHITAKE ISHII,[3] GEN MURAKAMI,[3,4] JOSÉ FRANCISCO RODRÍGUEZ-VÁZQUEZ,[5] AND SHIN-ICHI ABE[3]

[1]*Department of Histology and Developmental Biology, Tokyo Dental College, Tokyo, Japan*
[2]*Department of Neurology, Wonkwang University School of Medicine and Hospital, Institute of Wonkwang Medical Science, Iksan, Jeonbuk, South Korea*
[3]*Department of Anatomy, Tokyo Dental College, Tokyo, Japan*
[4]*Division of Internal Medicine, Jikoukai Home Visits Clinic, Sapporo, Japan*
[5]*Department of Anatomy and Human Embryology, Institute of Embryology, Faculty of Medicine, Complutense University, Madrid, Spain*

There seems to be no complete demonstration of the suboccipital fascial configuration. In 30 human fetuses near term, we found two types of candidate myodural bridge: (1) a thick connective tissue band running between the rectus capitis posterior major and minor muscles (rectus capitis posterior major [Rma], rectus capitis posterior minori [Rmi]; Type 1 bridge; 27 fetuses); and (2) a thin fascia extending from the upper margin of the Rmi (Type 2 bridge; 20 fetuses). Neither of these bridge candidates contained elastic fibers. The Type 1 bridge originated from: (1) fatty tissue located beneath the semispinalis capitis (four fetuses); (2) a fascia covering the multifidus (nine); (3) a fascia bordering between the Rma and Rmi or lining the Rma (13); (4) a fascia covering the inferior aspect of the Rmi (three); and (5) a common fascia covering the Rma and obliquus capitis inferior muscle (nine). Multiple origins usually coexisted in the 27 fetuses. In the minor Type 2 bridge, composite fibers were aligned in the same direction as striated muscle fibers. Thus, force transmission via the thin fascia seemed to be effective along a straight line. However, in the major Type 1 bridges, striated muscle fibers almost always did not insert into or originate from the covering fascia. Moreover, at and near the dural attachment, most composite fibers of Type 1 bridges were interrupted by subdural veins and dispersed around the veins. In newborns, force transmission via myodural bridges was likely to be limited or ineffective. The postnatal growth might determine a likely connection between the bridge and headache. Clin. Anat. 32:914–928, 2019.

Key words: fetuses; atlas; cervical; cervical vertebra axis; pachymeninx; elastic fibers; cervicogenic headaches

*Correspondence to: Kwang Ho Cho, Department of Neurology, Wonkwang University School of Medicine and Hospital, Institute of Wonkwang Medical Science, 895, Muwang-ro, Iksan-si, Jeollabuk-do 54538, South Korea. E-mail: neurlogy@wonkwang.ac.kr, neuro20015@gmail.com

This study was supported by a Grant-in-Aid for Scientific Research (no. 90733767: M.Y.) from the Ministry of Education, Culture, Sports, Science and Technology, Japan and by the Private University Research Branding Project from MEXT, Japan.

Received 17 April 2019; Revised 14 May 2019; Accepted 20 May 2019

Published online 10 June 2019 in Wiley Online Library (wileyonlinelibrary.com). DOI: 10.1002/ca.23411

INTRODUCTION

The myodural bridge, a connection between the spinal dura mater and suboccipital muscles, has been a focus of interest to orthopedic surgeons, neurologists, and anatomists for the last 20 years (reviewed by Kahkeshani and Ward, 2012), although the concept may encompass multiple structures such as the meningovertebral ligament (Scali et al., 2015), the vertebrodural ligament (Zheng et al., 2014), and the posterior epidural ligament (Shinomiya et al., 1996). Additional histological evidence for this structure has been provided by three groups (Pontell et al., 2013; Venne et al., 2017; Zheng et al., 2018). However, the figures they presented did not always include details of the histological connection of the bridge to the muscle-covering fascia or tendon. Moreover, there seems to be no or few histological demonstrations of the entire configuration of suboccipital fascial structures including the bridge. Rather than macroscopic observations, histological demonstrations are critically important to understand the fascial configuration because a dissection or surgical maneuver provides artifact structures such as a fibrous band or ligament (Range and Woodburne, 1964; Yabuki, 2016). Hereafter, the term "myodural bridge" is defined as a dura mater- or atlanto-occipital membrane-attached connective tissue band (1) originating from covering fasciae (comprising Type I collagen) of suboccipital muscles and/or (2) showing a direct and straight continuation of the striated muscle fibers. It appears that previous studies made little attempt to identify the "straight line" or vector of tension from the muscle fiber to the dura mater, despite the fact that this arrangement is essential for force transmission in a striated muscle-tendon interface (Huijing, 1999; Trotter, 1993). Without the force transmission along a straight line, fibroblasts do not provide a tendon in fetal development and later growth (Stopak and Harris, 1982; Mackey et al., 2008). Without a tendon, the muscle is not able to act on the target. Although these rules or mechanical demands are simple, previous studies on a fascial structure are liable to omit descriptions at higher magnification on the direction, attachment, and continuation of fibrous tissues: a good example is found in pelvic floor connective tissues (reviewed and criticized by Hinata and Murakami, 2014).

Using late-stage human fetuses near full term, we have previously investigated the fascial configuration in the limbs (Cho et al., 2018a,b), neck (Katori et al., 2012; 2013), and retroperitoneal region (Kinugasa et al., 2008; Matsubara et al., 2009). At the stage, collagen and elastic fibers are well differentiated and can be easily discriminated using routine staining techniques (Kinoshita et al., 2013; Kinugasa et al., 2012). At the late fetal stage, a muscle-covering fascia is established even in the thigh, exhibiting a specific multilayered configuration (Cho et al., 2018b). Histological investigation of soft tissues in such large fetuses has several advantages: (1) the fascial configuration is the same as or similar to that in adults in most regions of the body; (2) pathological changes in the fascia, such as adhesion and thickening with inflammation, are minimal or absent; (3) preparation of tissue sections is much easier than for adult specimens because of the smaller size of the structures and minimal degree of calcification. We have also used fetal specimens for investigation of the neurodural junction in the thoracic spinal cord (Cho et al., 2016). Moreover, we have become familiar with the topographical anatomy of the atlanto-occipital region through our recent study of a temporary disk-like structure appearing at the median atlanto-axial joint (Sakanaka et al., 2019). Consequently, using human fetuses near term, the aim of this study was to demonstrate the morphology and individual variations in the suboccipital fascial configuration including the myodural bridge candidate.

MATERIALS AND METHODS

The study was performed in accordance with the provisions of the Declaration of Helsinki 1995 (as revised in Edinburgh 2000). We observed sagittal sections of 30 human fetuses near term (crown-rump length [CRL] 250–310 mm; gestational age 30–37 weeks; Table 1). All specimens were part of the large collection kept at the Department of Anatomy and Embryology of the Universidad Complutense, Madrid, and had originated from miscarriages and ectopic pregnancies at the Department of Obstetrics of the University. The use of these specimens was approved by Complutense University ethics committee (B08/374). Most sections had been stained with hematoxylin and eosin, while some of the unstained sections were newly subjected to Elastica-Masson staining (a variation of Masson-Goldner staining; Motohashi et al., 1995; Hayashi et al., 2010), for demonstration of elastic fibers. Most photographs were taken with a Nikon Eclipse 80, whereas photographs at ultra-low magnification (objective lens less than $\times 1$) were obtained using a high-grade flat scanner with translucent illumination (Epson scanner GTX970). In the present histology, the ligamentum nuchea was used for positive control of the elastic fiber staining, while muscle attachments to the atlas (AT) and axis (AX) were used for positive control of collagen fiber bundles connecting between a striated muscle fiber and it target.

A major proportion of the present specimens had been used for our recent study of a temporarily appearing disk in the median atlanto-axial joint (Sakanaka et al., 2019). The present specimens had been stored in formalin solution for more than 10 years. In the Department of Anatomy and Embryology, Complutense University, Madrid, the dissection for preparation of histological specimens was performed by two experienced specialists for human fetal anatomy (G.M. and J.F.R-V), who interpreted all slides each other and reached a conclusion together thus eliminating the possibility of interobserver bias during 2016–2018 and histological procedures were performed by technicians in the Department. The other two (M.Y., K.K.) observed sections and took photos. During the histological process, macroscopic observations were impossible for the preservation of the connective tissue around the AT and AX because the target structures are located deeply near the midsagittal plane. Although the numbers

TABLE 1. Summary of Candidates Myodural Bridge We Found

CRL (mm)	ATd (mm)	Rmi upper	Type 1 candidates	
250	26	+	Rma	
258	26	+	Rma	
290	26	+	Rma, Rma + Oci	
297	28	–		
300	28	+	Rma/Rmi	
261	29	+	Rma, Rmi lower	
265	29	–	Rma, Rma + Oci, MU	
268	29	+	Rma, Rma/Rmi	
275	29	–	Rma/Rmi, MU	
278 (Fig. 4)	30	–	Rma, MU	
302	30	+	Rma/Rmi, MU	
280	31	+	Rma/Rmi	
282	31	–		
285	31	–		
287 (Fig. 4)	32	+	Rma/Rmi, MU	
291	32	+	Rma, Rmi lower	Asymmetrical
292	33	–	Rma, MU	
293	33	+	Rma + Oci	
294	33	–	Fat, Rma	
296	34	+	Rma + Oci, Rmi lower	
299 (Fig. 5)	34	–	Rma, Rmi lower	
301	35	–	Rma/Rmi	
270	35	+	Rma/Rmi	
255	35	+	Rma + Oci, Rmi lower	
304 (Fig. 5)	36	+	Rma + Oci, MU	
305	38	+	Fat, MU	
260	40	+	Fat, Rma	
279	40	–	Rma + Oci, Rma	
307	40	+	Rma, MU	
310 (Figs. 2 and 3)	41	+	Fat	Asymmetrical

ATd: the maximum diameter of the atlas at the insertion of the rectus capitis posterior minor muscle.
Rmi upper (Type 2 bridge candidate) or Rmi lower: fascial connection from upper or lower parts of the rectus capitis posterior minor.
Rma, OCi: a connection with a covering fascia of the rectus capitis posterior major or the obliquus capitis inferior; Rma/Rmi: a fascia bordering the rectus capitis major and minor muscles; Fat, a connective tissue band from a fatty tissue beneath the semispinalis capitis; MU, a fascia from the multifidus.
Asymmetrical indicates that the sagittal planes were slightly tilted.

of specimens were limited to 30, this was all with good preservation of upper cervical tissues.

Using SPSS 21.0 (IBM, Armonk, NY), spearman correlation coefficient was estimated to determine the linear association between the maximum diameter of the AT posterior arch and CRL. The outcome results were interpreted according to the degree of association as strong (=0.7–1), moderate (=0.5–0.7), or low (=0.3–0.5) after taking significant correlation ($P < 0.05$) values into consideration.

RESULTS

The present sagittal sections allowed good visualization of the topographical anatomy of the inferior end of the occipital bone (occiput), posterior parts of the AT and AX, the joint cavities and the suboccipital muscles, that is, the rectus capitis posterior major (Rma) and minor muscles (Rma, rectus capitis posterior minori [Rmi]), and the obliquus capitis inferior muscle (Oci). We found no anomalies at the craniocervical junction such as Chiari malformations and neurocentral synchondrosis. However, we found marked individual variations in distance among the occiput, AT and AX, and these values were not correlated with the age or CRL of the fetuses (details to be submitted in a separate paper). In contrast, the maximum diameter of the AT posterior arch ranged from 26 to 41 mm at the origin of the Rmi was significantly correlated with the CRL ($r = 0.36$, $P < 0.05$). In addition, the transverse atlantis and alar ligaments appeared to develop normally, in contrast to our previous observations of early fetuses (Abe et al., 2012).

To ascertain whether or not a morphological basis for force transmission from a striated muscle to the target had already become established, we first observed the muscle insertion to, or origin from, the AT or AX (Fig. 1). In the Rma, Rmi, and Oci of all 30 fetuses examined, we found a direct continuation along a straight line between the striated muscle fibers and the composite collagen fibers of the periosteum or perichondrium. Rather than suboccipital muscles, the composite collagen fibers were most evident at an insertion of the MU muscle to the AX, where sagittal sections demonstrated collagen fibers arranged in parallel over the entire interface between the muscle and the

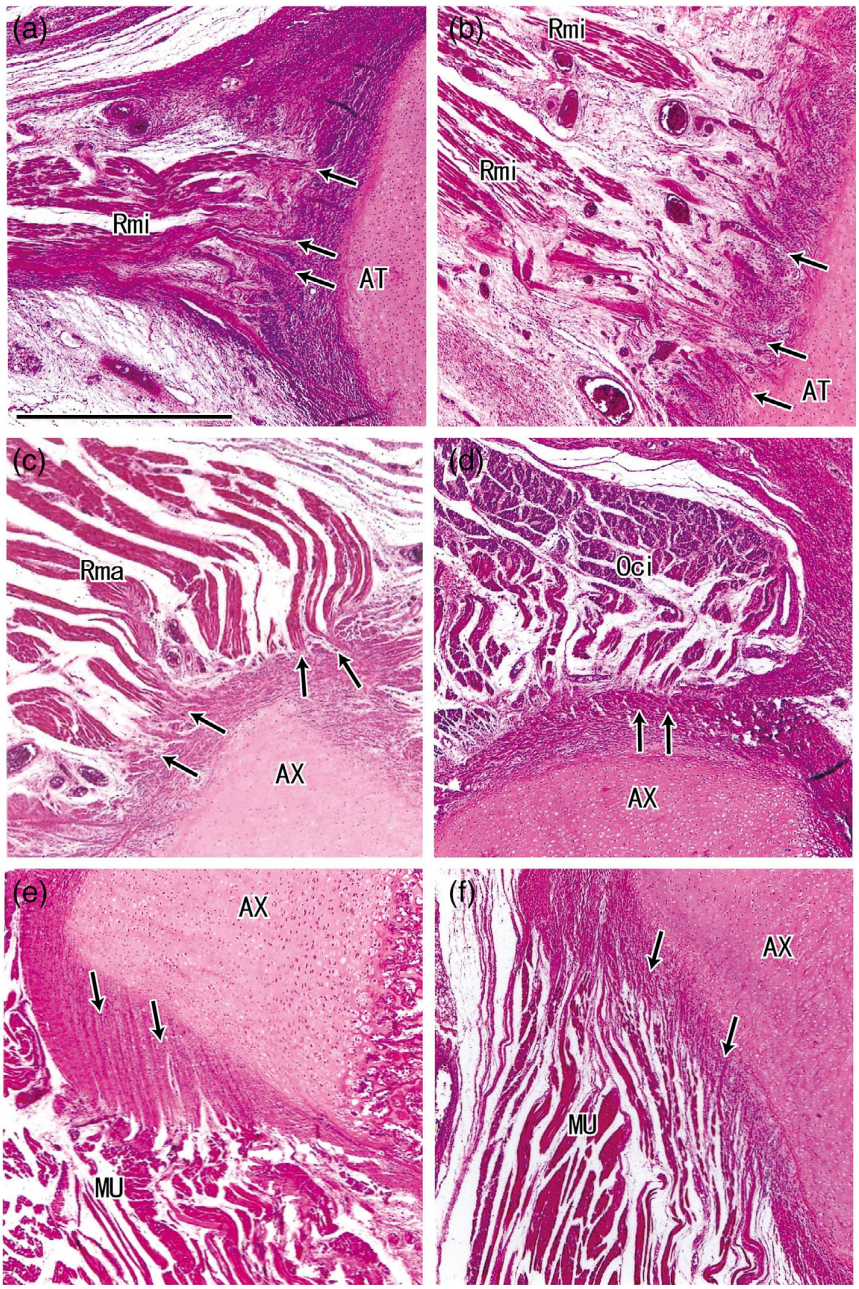

Fig. 1. Striated muscle fiber insertion to, or origin from, periosteum or perichondrium. Panels (**A**) and (**B**) display the origin of the rectus capitis posterior minor (Rmi) from the atlas. Panel A (or Panel B) is a higher-magnification view of the upper part of Figure 4A (or Fig. 5A). Panel (**C**) shows the origin of the rectus capitis posterior major (Rma) from the axis (AX) and is a higher-magnification view of the lower part of Figure 4G. Panel (**D**) a higher-magnification view of the lower part of Figure 3C, showing the origin of the obliquus capitis inferior (Oci) from the AX. Panels (**E**) and (**F**) show the insertion of the multifidus to the AX and are higher-magnification views of the lower part of Figure 5D and Figure 6C, respectively. All panels were prepared at the same magnification (scale bar in Panel A, 1 mm). [Color figure can be viewed at wileyonlinelibrary.com]

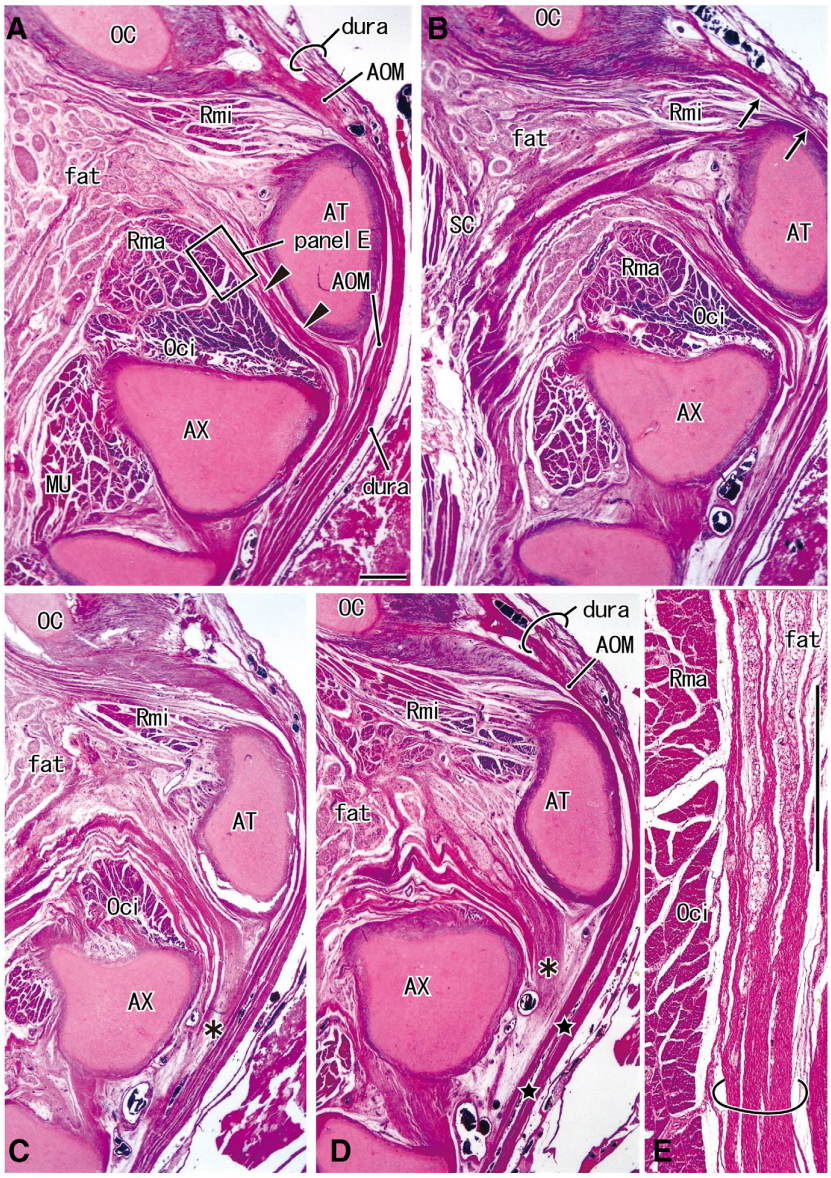

Fig. 2. Myodural bridge candidates in a fetus of 310 mm crown-rump length. Panel (**A**) (or Panel **D**) displays the most lateral or right (or medial) site in the figure. Panel (**E**) is a higher-magnification view of the square in Panel A. Intervals between panels are 0.4 mm (A, **B**; B, **C**) and 0.3 mm (C–D). Sections of the contralateral side will be shown in Figure 2. The dura mater appears to be multilaminar above the atlas (Panel A). A covering fascia along the upper margin of the Rmi extends anteriorly to join the posterior membrane (arrows in Panel B). A thick connective tissue band (arrowheads in Panel A) originates from fatty tissue beneath the semispinalis capitis muscle (SC) and runs anteriorly to merge with the posterior atlanto-occipital membrane. At medial or median sites, composite fibers of the band disperse in the epidural space (asterisk in Panels C and D). The atlanto-occipital membrane is separated from the dura mater by a narrow space (stars in Panel D). Striated muscle fibers of the Rma and Oci do not attach to the covering fascia (semicircle in Panel E). Panels A–D were prepared at the same magnification: scale bars in Panels A and E, 1 mm. For other abbreviations, see the list of common abbreviations. [Color figure can be viewed at wileyonlinelibrary.com]

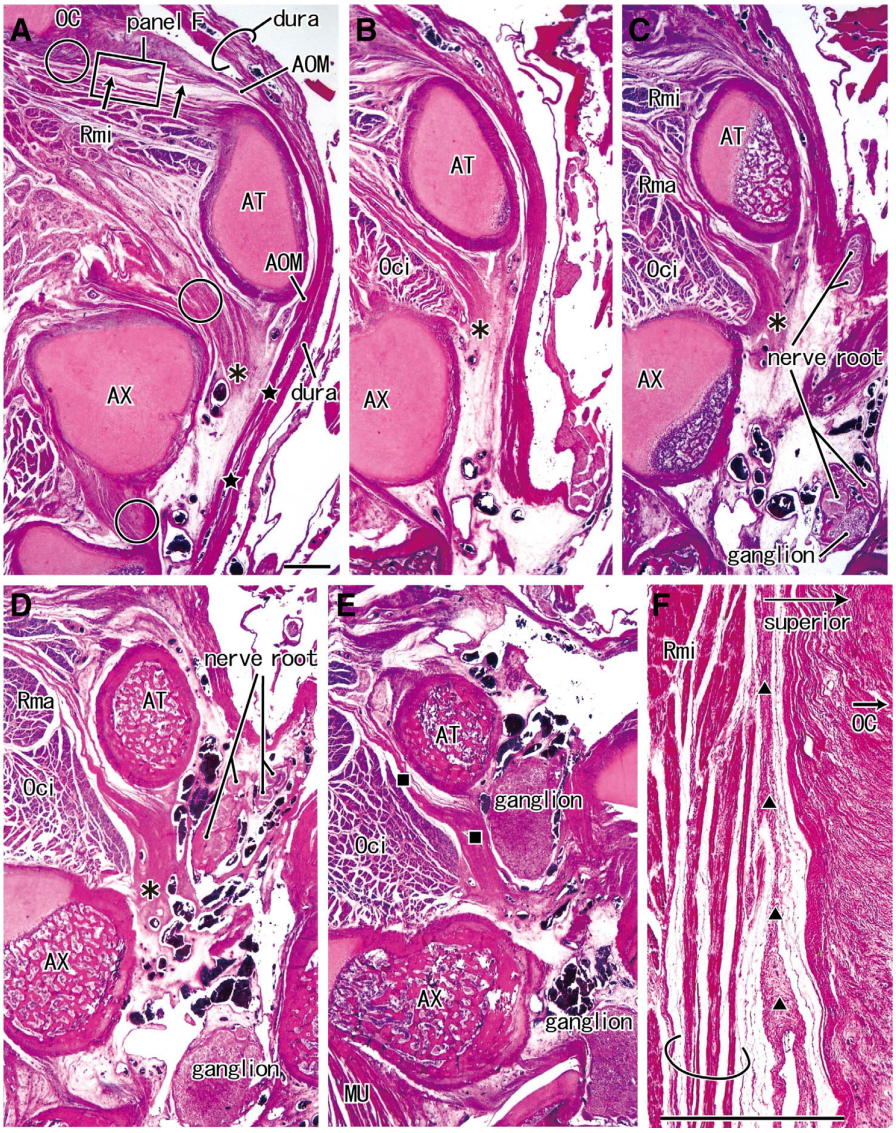

Fig. 3. Myodural bridge candidates and spinal nerve roots in a fetus of 310 mm CRL (the side contralateral to that in Fig. 1). Panel (**A**) (0.4 mm to the left of Fig. 1D) almost corresponds to the midsagittal plane, while Panel (**E**) shows the most left lateral site in the figure. Panel (**F**) is a higher-magnification view of the square in Panel A. Intervals between panels are 0.8 mm (A, **B**), 0.6 mm (B, **C**), and 0.7 mm (C, **D**; D, E). A covering fascia along the upper margin of the Rmi extends anteriorly to join the posterior atlanto-occipital membrane (arrows in Panel A). The atlanto-occipital membrane is separated from the dura mater by a narrow space (stars in Panel A). At the lateral sites, composite fibers of a connective tissue band (Fig. 1A) disperse in the epidural space (asterisks in Panels A–D) and partly join the dura mater around the spinal ganglion and nerve roots (squares in Panel E). The upper fascia of the Rmi (triangles in Panel F) differs in direction from the tendons and striated muscle fibers (semicircle in Panel F). Elastic and collagen fibers in the three circles in Panel A are shown in Figure 7. Panels A–E were prepared at the same magnification: scale bars in Panels A and F, 1 mm. For other abbreviations, see the list of common abbreviations. [Color figure can be viewed at wileyonlinelibrary.com]

perichondrium (Fig. 1E,F). Consequently, in any given fetus, an effective tendon-hard tissue interface had been established for three suboccipital muscles examined.

In some specimens (two fetuses; "asymmetrical" in Table 1), the suboccipital muscles appeared not to exhibit left–right symmetry (Figs. 2 and 3). This may have been because of slight tilting of the sectional plane, such as a slight leftward shift at the anterior end in combination with a slight rightward shift at the posterior end. In slightly tilted planes, the Oci was seen together with the medially located origins of the Rma or Rmi. The tilted sagittal planes allowed observation of the topographical relationship between laterally located nerve roots and the candidate myodural bridge (Fig. 3D,E).

The posterior atlanto-occipital membrane (AOM) appeared to end at the posterior arch of the AT (Figs. 4 and 5) or extend to the inferior end of the occiput (Figs. 2–3, and 6), whereas the dura mater always extended further superiorly along the internal aspect of the occiput. In the suboccipital region, the posterior membrane was attached to the dura mater, but sometimes the two were separated by a narrow space (Figs. 2D, 3A, and 4A,F). Rather than extending along the internal aspect of the occiput, the posterior membrane sometimes appeared to extend posterosuperiorly, continuing to the occipital periosteum along the upper aspect of the Rmi (Figs. 2A and 6A). Above the AT, the dura mater was usually identified as double laminae sandwiching veins (Figs. 3B and 4A, E), but sometimes it was multilaminar (Figs. 2A and 6A). However, below the AT, the posterior membrane was often difficult to discriminate from the external lamina, since veins were also likely to exist between the posterior membrane and the dura mater.

Superior to the Rma or Oci, a thick connective tissue band was evident, representing the most likely candidate for the myodural bridge (Type 1 bridge; 27 fetuses; Table 1). This connective tissue band ran anteriorly to merge with the AOM or dura mater (Figs. 2A, 4A,G, 5D, and 6B,C). The band originated from fatty tissue located beneath the semispinalis capitis muscle (four fetuses; Fig. 2A), a fascia covering the MU muscle (nine fetuses; Figs. 4A and 6B), or a fascia bordering between the Rma and Rmi (eight fetuses; Fig. 4G). The connective tissue band also likely originated from a fascia covering the Rma (five fetuses; Fig. 5D), the lower aspect of the Rmi (three fetuses; Fig. 5A,F), or the Rma and Oci together (nine fetuses; Fig. 6A,C). Depending on the site (median, medial, or lateral), multiple origins of the Type 1 band were likely to coexist in the 27 fetuses, for example, "Rma/Rmi, MU" (a fascia between the Rma and Rmi, another fascia covering the MU) in three specimens (CRL 275, 302, and 287 mm) in Table 1.

Laterally, composite fibers of the Type 1 candidate or connective tissue band became dispersed in the dura mater around and near the spinal ganglion, nerve roots, and epidural veins (Figs. 2C,D, 3A–D, and 6D,F). However, there was no or little histological evidence that striated muscle fibers were connected with a fascia covering the muscle or the connective tissue band (Figs. 2E, 3F, 4D,H, and 5G). For instance, as shown in Figure 4H, striated muscle fibers of the Rma were oriented vertically to the direction of the intermuscular band, while some of the Rmi fibers originated from a fascia other than the band. Otherwise, as shown in Figure 5G, the band along the Rma and Oci contained abundant veins in spite of the expected force transmission along it. In one limited sample, a fascia covered the Rma, into which a bundle of striated muscle fibers inserted (Fig. 6G).

The Type 2 candidate of the myodural bridge was found in a fascia extending from the upper margin of the Rmi to the AOM or dura mater (Type 2 bridge; 20 fetuses; Figs. 2B, 3A, 4F,G, and 6A; Table 1). A small proportion of the muscle fibers appeared to connect with the upper fascia (Figs. 4E and 6E). Conversely, almost all of the striated muscle fibers of the Rmi originated from the posterior arch of the AT via collagen fibers from the perichondrium. (Fig. 1A,B). The upper fascia of the Rmi was much thinner than the aforementioned Type 1 band because of a narrow space above the Rmi. Similarly to the upper margin, there was a fascia liming the lower aspect of the Rmi ("Rmi lower" in Table 1), but it merged with a thick fibrous band running between the Rmi and Rma. Thus, "Rmi lower" is classified into Type 1 bridge candidate in Table 1. As shown in Figure 5F, the striated muscle fibers of the Rmi were sometimes attached to the lower fascia, but the latter became separated from the candidate bridge candidate anteriorly. In lateral sections, the spinal nerve roots passed through the dural sac and the ganglion and venous plexus were surrounded by a lateral continuation of the dura mater (Figs. 3C–E, 5D,E, and 6D,F).

Although we observed the typical insertion and origin of striated muscles in which a muscle fiber and a collagen fiber were arranged in parallel and along a straight line (Fig. 1), such a configuration was not found at the dural terminal of candidate myodural bridges. None of these bridge candidates contained elastic fibers, in contrast to the ligamentum nuchae (Fig. 7), in which the elastic fiber configuration varied among fetuses: (1) a parallel arrangement in the sagittal plane (22 fetuses; Fig. 7G); (2) an oblique or vertical array in the sagittal plane (six fetuses; Fig. 7A); or (3) an early stage in which short elastic fibers were irregularly scattered (two fetuses; Fig. 7D). When the ligamentum nuchae was defined as a structure containing abundant elastic fibers, we did not find any connection between it and the candidate myodural bridge.

Overall, we found candidate myodural bridges in 27 of 30 fetuses (Fig. 8 and Table 1): (1) a thick connective tissue band running between the Rma and Rmi (Type 1 bridge) and/or (2) a thin fascia running along the upper margin of the Rmi (Type 2 bridge). However, there was little evidence for straight transmission of force from the suboccipital muscles because of: (1) the presence of dispersed or loose composite fibers near the target; (2) veins interrupting or embedded in the bridge candidate; and (3) no or few striated muscle fibers originating from or inserting to the muscle-covering fascia connected to the bridge candidate.

DISCUSSION

Below the AT, the AOM was often difficult to discriminate from the external lamina of the spinal dura mater. Thus, although the term "myodural bridge" indicates a fibrous tissue connecting between the suboccipital muscle and dura mater, it was difficult to trace the connective tissue band to the dura mater even in clear histological sections. In this section, we will state about no or few connections between the muscle fiber and covering fascia: for an effective bridge, the latter should be continuous with the connective tissue band toward the dura mater. Therefore, in the present study, the term "myodural bridge" was usually no more than the candidate (Fig. 8). The figures presented here appear to demonstrate the myodural bridge candidates more clearly than previous histological studies using adult specimens.

Depending on the origins and course, we classified candidate myodural bridges into two types (Fig. 8):

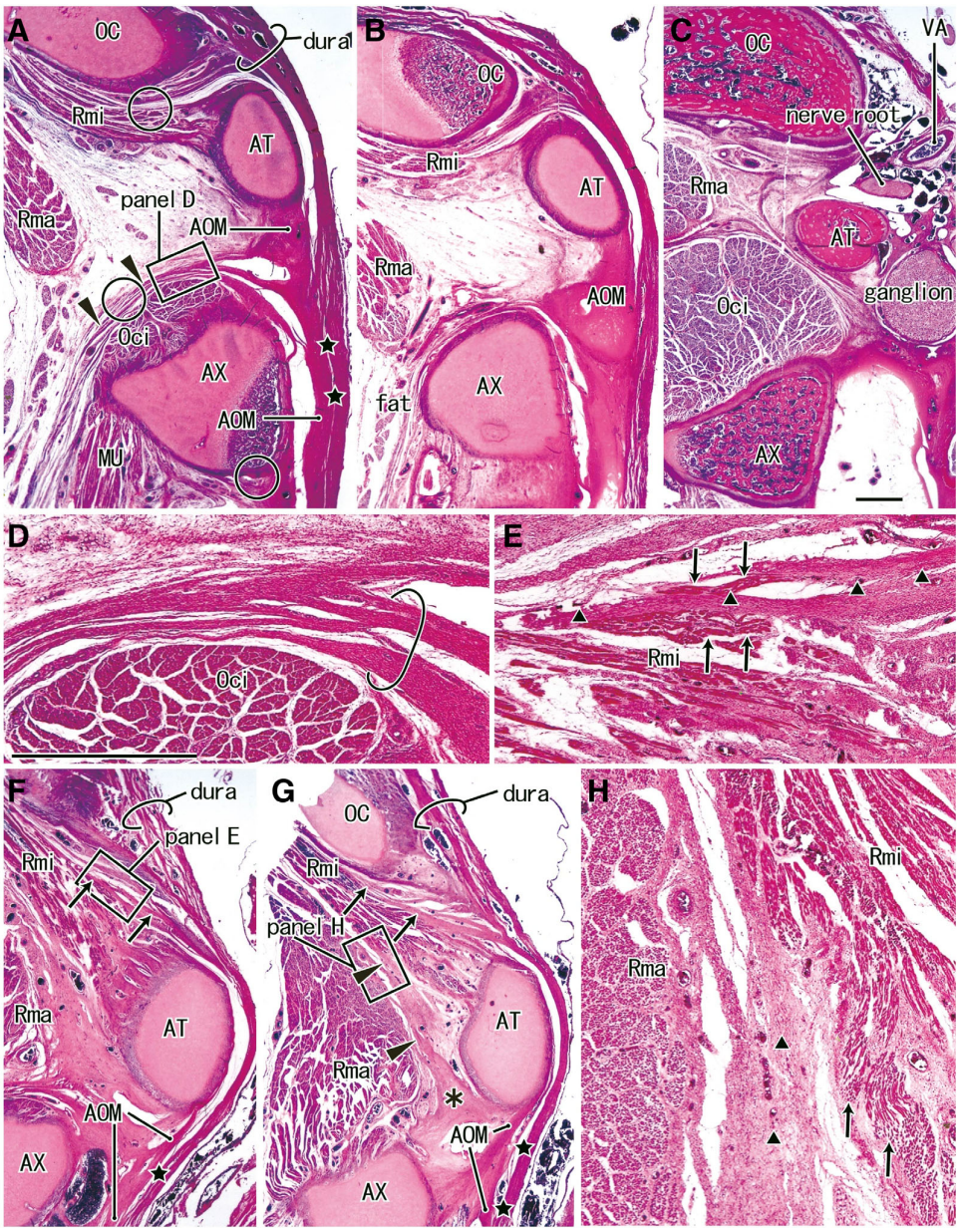

Fig. 4. Legend on next page.

(1) the Type 1 bridge composed of a thick connective tissue band with various origins and running below the Rmi (27 fetuses); and (2) the Type 2 bridge originating from a thin fascia extending along the upper aspect of the Rmi (20 fetuses). Thus, such candidates were often present both above and below the Rmi. On the basis of macroscopic observations, Zumpano et al. (2006) classified the upper fascia of the Rmi into three categories: (1) no attachment to the AOM; (2) continuity of the Rmi tendon with the membrane; and (3) the Rmi-covering fascia continuous with the membrane. Their photos suggested that the second and third categories, a tendon and a covering fascia, corresponded to the present Type 2 bridge. Their third category, a covering fascia running along the upper aspect of the Rmi, was clearly demonstrated by Nash et al. (2005) in an image of an elegantly prepared confocal E12 sheet plastination specimen, but the photo did not include the site of merging with the AOM. Venne et al. (2017) also demonstrated the present Type 2 bridge histologically by Masson trichrome staining. Nevertheless, the present study seemed to first demonstrate the histology in fetuses near term: the morphologies were most likely to be similar to the myodural bridge in newborns.

A connective tissue band running along the lower aspect of the Rmi (one of the present Type 1 bridges) has also been described on the basis of routine histology (Pontell et al., 2013; Zheng et al., 2018) and P45 sheet plastination (Zheng et al., 2014). These descriptions suggested that the origins of the bridges or fasciae were the Oci, the Rma and the lower aspect of the Rmi. In the photos, however, we were unable to clearly identify any connection between the bridge and the dura mater or the atlanto-occipital membrane. Notably, previous histological studies did not demonstrate any coexisting multiple bridge candidates with different origins, for example, a thick Type 1 bridge running between the Rmi and Rma and a thin Type 1 bridge above the Rmi: In adults, histological demonstration of the myodural bridge appears to be very difficult. Moreover, none of the above studies drew attention to any connection between the striated muscle fibers and the covering fascia. When a striated muscle fiber runs vertically to a straight line or vector from the covering fascia, via a bridge candidate to the dura mater, any force transmission role would seem to be very limited. Morphologically, any effective connection would be a muscle-target interface in which muscle and collagen fibers run parallel and in the same direction as demonstrated in the Results section (Fig. 1).

In effective attachments of striated muscle fibers, any muscle-covering fascia would play a role in pulling up the target, including the skeleton: a well-known example is the tensor fasciae latae and gluteus maximus muscles, which allow strong stretching of the iliotibial band for lateral knee stabilization (Gerlach and Lierse, 1990). In contrast to the striated muscle fibers oriented along the supero-inferior AX of the lower extremity to reach a developing iliotibial band (Cho et al., 2018b; Shiraishi et al., 2018), muscle fibers of the Rma and Oci differed in direction from the candidate Type 1 myodural bridges, the latter of which requires a pull-up vector. Thus, the power of muscle contraction was most likely conducted to collagen fibers in the bridge after a reduction and change of direction. However, this indirect conduction of force appears to be important for avoiding injury to the spinal nerve roots. Similar examples have been described at soft tissue-striated muscle interfaces, that is, the extraocular rectus muscle pulley (Demer et al., 1995; Kono et al., 2002) and the levator ani muscle insertion to the urethra, vagina and rectum (Hinata and Murakami, 2014; Sasaki et al., 2014). Notably, in both direct and

Fig. 4 Myodural bridge candidate from the multifidus in a fetus of 278 mm crown-rump length (CRL) and coexistence of multiple candidates in a fetus of 287 mm CRL. Panels (**A**–**D**) display sections from a fetus of 278 mm CRL, while Panels (**E**–**H**) show sections from a fetus of 287 mm CRL. Panels A and F display the most medial site in each specimen. Panel D is a higher-magnification view of the square in Panel A, while Panels E and H are higher-magnification views of the squares in Panel F and G, respectively. Intervals between panels are 0.5 mm (A, B) and 0.8 mm (B, C; F, G). A thick connective tissue band (arrowheads in Panel A) originates from a fascia covering the multifidus muscle (Panel A) via the upper surface of the Oci to merge with the posterior atlanto-occipital membrane. Striated muscle fibers of the Oci are separated from the band (Panel D). A fascia running along the upper margin of the Rmi (arrows in Panel F) connects with the atlanto-occipital membrane. A proportion of the striated muscle fibers of the Rmi (arrows in Panel E) join the fascia (triangles in Panel E). Another thick fascia bordering between the Rma and Rmi (arrowheads in Panel G) appears to disperse near the atlanto-occipital membrane (asterisk). Striated muscle fibers in the lower part of the Rmi (arrows in Panel H) appear to originate from a fascia other than the bridge candidate (triangles in Panel H). Muscle fibers of the Rma are oriented vertical to the bridge candidate (Panel H). The atlanto-occipital membrane is separated from the dura mater by a narrow space (stars in Panels A, F, and G). Elastic and collagen fibers in the three circles in Panel A are shown in Figure 7. Panels A–C, F, and G or Panels D, E, and H were prepared at the same magnification: scale bars in Panels C and D, 1 mm. For other abbreviations, see the list of common abbreviations. [Color figure can be viewed at wileyonlinelibrary.com]

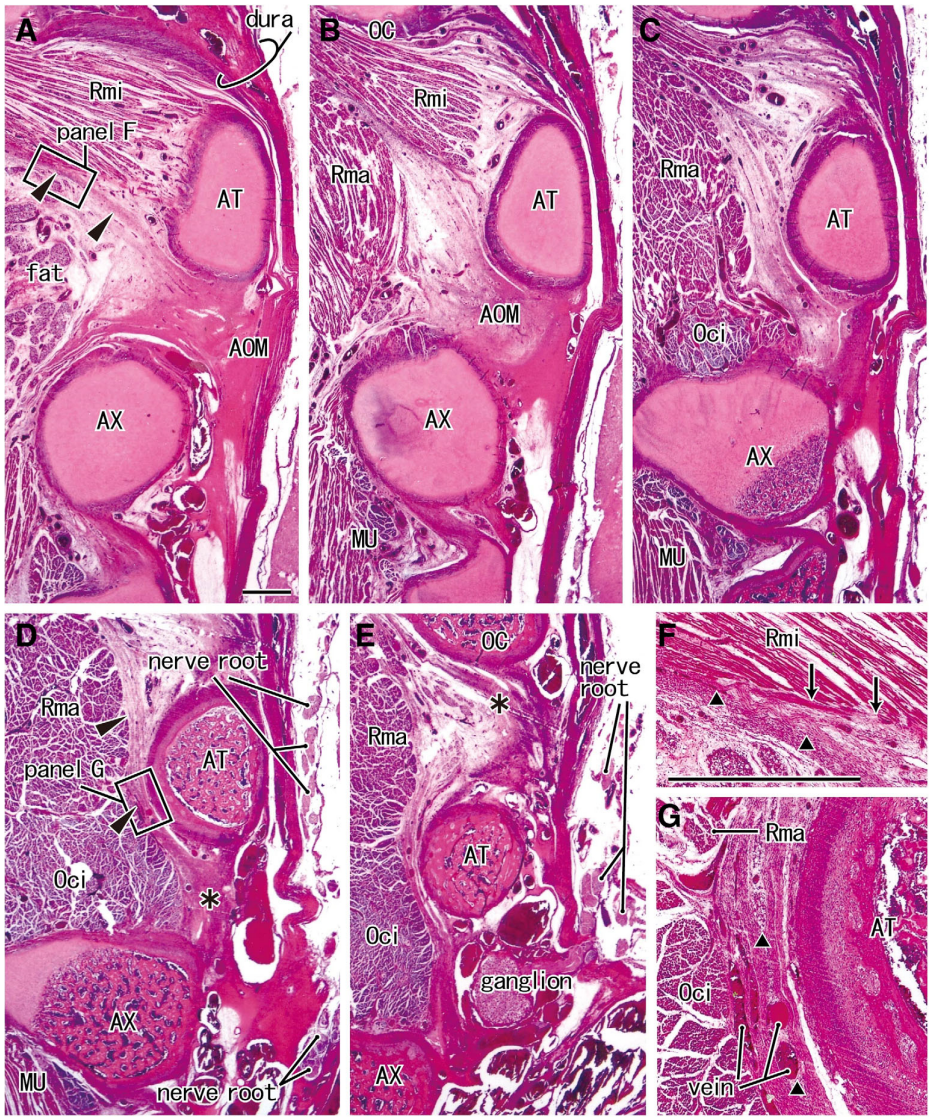

Fig. 5. Multiple candidates for the myodural bridge in a fetus of 299 mm crown-rump length. Panel (**A**) (or Panel **E**) displays the most medial (or lateral) site in the figure. Panels (**F**) and (**G**) are higher-magnification views of the squares in Panels A and G, respectively. Intervals between panels are 1.4 mm (A, **B**), 0.9 mm (B, **C**; C, **D**), and 1.0 mm (D, E). A thick fascia running mostly along the lower margin of the Omi (arrowheads in Panel A) connects with the atlanto-occipital membrane. This fascia (triangles in Panel F) differs in direction from the linear origin of the Omi muscle fibers (arrows in Panel F). Another thick fascia (arrowheads in Panel D) originates from a common covering fascia of the Rmi and Oci and disperses near the nerve root (asterisks in Panels D and E). The fascia (triangles in Panel G) contains abundant veins. Panels A–E and Panels F and G were prepared at the same magnification: scale bars in Panels A and F, 1 mm. For other abbreviations, see the list of common abbreviations. [Color figure can be viewed at wileyonlinelibrary.com]

indirect transfer of striated muscle contraction, a collagen fiber mesh (Eng et al., 2015) and/or elastic fibers (Kim et al., 2015; Osanai et al., 2009) contribute to a gradual release of tension, thus limiting the peak power of muscle contraction. Since the myodural bridge most likely carries no elastic fibers, any direct and straight

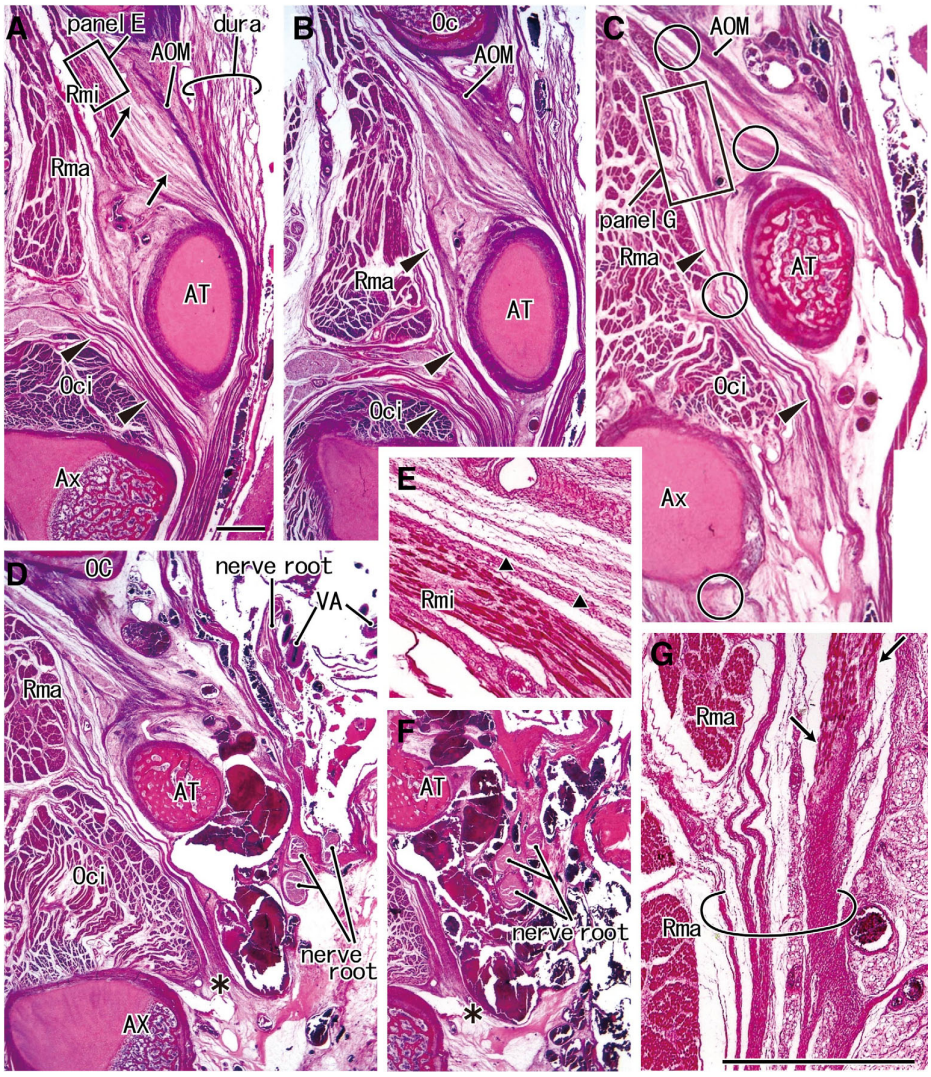

Fig. 6. Multiple candidates for the myodural bridge in a fetus of 304 mm crown-rump length. Panel (**A**) (or Panel **F**) displays the most medial (or lateral) site in the figure. Panels (**E**) and (**G**) are higher-magnification views of the squares in Panels A and (**C**) respectively. Intervals between panels are 0.7 mm (A, **B**), 0.9 mm (B, C), 1.5 mm (C, **D**), and 0.6 mm (D–F). A thin fascia mostly running along the upper margin of the Omi (arrows in Panel A) appears to join the atlanto-occipital membrane. The dura mater is multilaminar above the atlas. This thin fascia (triangles in Panel E) differs in direction from striated muscle fibers of the Omi. Other thick fasciae (arrowheads in Panels A–C) originated from fasciae covering the Rmi and Oci and merge with the atlanto-occipital membrane. A bundle of muscle fibers of the Rma (arrows in Panel G) originates from one of the fasciae (semicircle in Panel G). At the lateral sites, composite fibers of the bridge candidate disperse in the dura mater near the spinal ganglion and around the epidural veins (asterisks in Panels D and E). Elastic and collagen fibers in the four circles in Panel C are shown in Figure 7. Panels A–D and F, and Panels E and G, were prepared at the same magnification: scale bars in Panels A and G, 1 mm. For other abbreviations, see the list of common abbreviations. [Color figure can be viewed at wileyonlinelibrary.com]

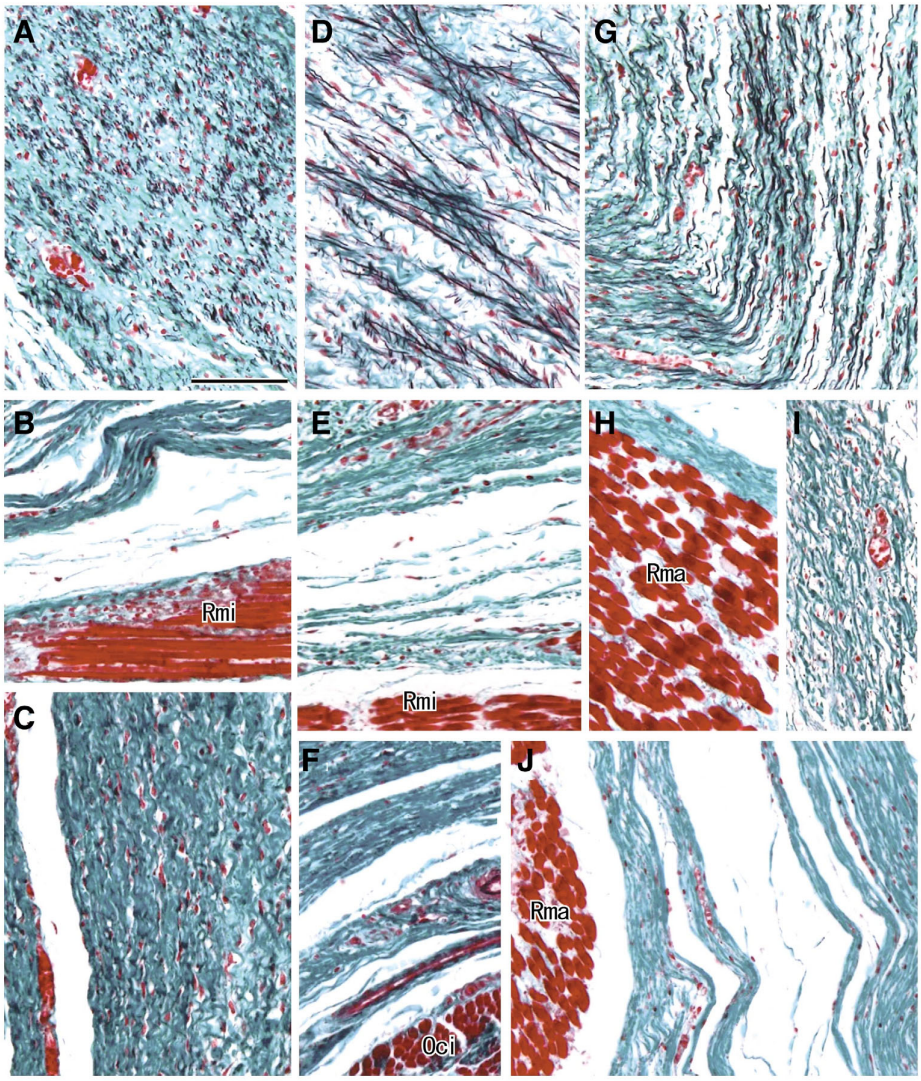

Fig. 7. Elastic and collagen fibers contained in the ligamentum nuchae and myodural bridge candidate. With elastica Masson staining, elastic fibers appear black, while collagen fibers appear green-blue. Black-colored elastic fibers are limited to the ligamentum nuchae: the ligament between the second and third vertebrae is shown in Panel (**A**) (crown-rump length [CRL] 310 mm), Panel (**D**) (CRL 278 mm), and Panel (**G**) (CRL 304 mm). The elastic fibers run obliquely or vertically to the sagittal plane (Panel A), or run almost parallel (Panel G). In Panel D, however, they are short and irregular. Panels A–C display higher-magnification views of the three circles in Figure 3A, respectively: Panel (**B**) a fascia running along the upper aspect of the Rmi; Panel (**C**) a connective tissue band running antero-inferiorly between the atlas and the axis. Panels D–F exhibit higher-magnification views of the three circles in Figure 4A, respectively: Panel (**E**) a fascia running along the upper aspect of the Rmi; Panel (**F**) a fascia running along the upper aspect of the Oci. Panels G–J show higher-magnification views of the four circles in Figure 6C, respectively: Panel (**H**) a fascia running along the anterosuperior aspect of the Rma; Panel (**I**) a connective tissue band originating from the anterosuperior aspect of the Rma; Panel (**J**) a fascia running along the Rma and Oci. All panels were prepared at the same magnification: scale bar in Panel A, 0.1 mm. [Color figure can be viewed at wileyonlinelibrary.com]

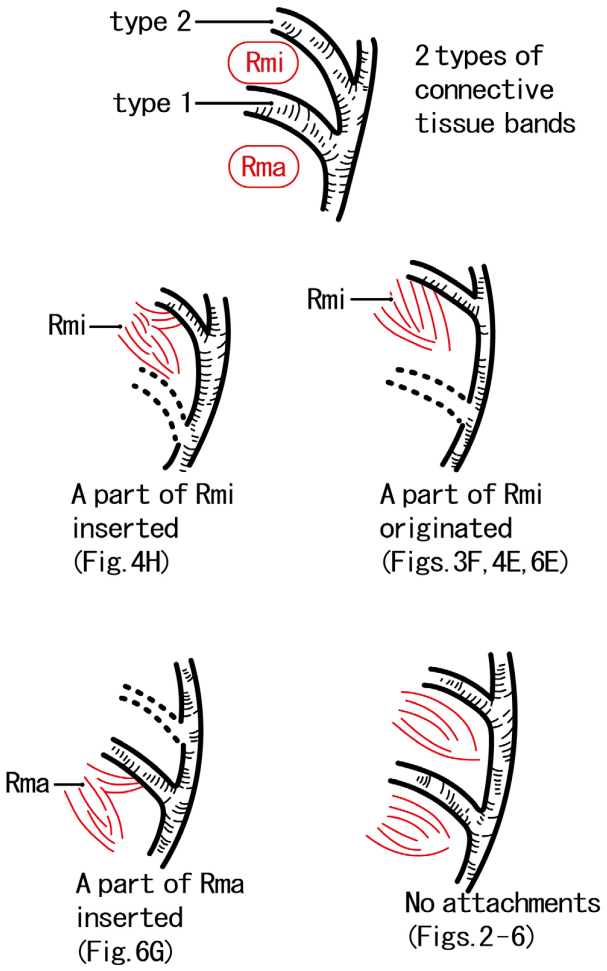

Fig. 8. Schematic representation of the present results. We found two types of connective tissue bands reaching the atlanto-occipital membrane or spinal dura mater: (1) Type 1 band passing between the rectus capitis posterior major and minor muscles (Rma, Rmi) and (2) Type 2 band along the upper margin of the rectus capitis posterior minor muscle (candidates of the myodural bridge). The Type 1 band was likely to pass between the obliquus capitis inferior and rectus minor muscles (variations in origin, see "Other bridge candidates" in Table 1). A small part of the rectus minor muscle was likely to insert into or originate from the Type 2 band (the second line of panels). Likewise, in a single specimen, a thin bundle of the rectus major muscle inserted into the Type 1 band (lowermost panel, left-hand side; see also Fig. 6G). However, in almost all specimens, there was no attachment between the striated muscle fiber and Type 1 connective tissue band (lowermost panel, right-hand side) because the muscle fiber did not insert into or originate from the covering fascia. [Color figure can be viewed at wileyonlinelibrary.com]

transmission of force from the striated muscle fibers to the dura mater would appear to pose a risk especially in young adults in which striated muscles obtain full power.

In this study, because we found candidate myodural bridges in 27 of 30 fetuses, we were able to conclude the bridge was likely to appear until the late stage of prenatal age in spite of the limited number of specimens examined. However, our observations were insufficient to provide proof of effective force transmission from the suboccipital muscles to the dura mater because of: (1) the presence of dispersed or loose composite fibers near the dura mater or atlanto-axial membrane; (2) a venous plexus or veins interrupting the bridge; and (3) no or few striated muscle fibers originating from or inserting to the muscle-covering fascia connected to the bridge. We could not rule out the possibility that the bridge was in the process of development or growth in the present specimens. In fact, in some fetuses, elastic fibers of the ligamentum nuchae indeed appeared to be developing and exhibited an irregular pattern. Like small muscles attached to the joint capsule, the myodural bridge might play a role in preventing impingement or infolding of the dura mater during extension of the upper cervical vertebrae as reviewed by (Kahkeshani and Ward (2012). The topographical relationships or alignments of the posterior components of the occiput–AT–AX showed marked individual variations. Therefore, such individual differences might determine the timing and sequence of development and growth of the myodural bridge. However, even in fetuses, it is well-known that striated muscle fiber insertions to the joint capsule are well established in the elbow and shoulder (Abe et al., 2011; Jin et al., 2016).

This study has some limitations: this is a single center study with relatively small sample size. However, this study method is not aimed at such statistical generalization, but an analytical one. Yuan et al. (2017) suggested that the chronic headache patients had hypertrophy of the Rmi, even though the cause-and-effective relation was unclear. Whenever pathological changes occurred in the deep muscles of suboccipital region, improper forces may be transmitted from myodural bridge to the pain-sensitive cervical dura mater, resulting in cervicogenic headache. Morphologies in fetuses near term seemed to strongly suggest those in newborns. Consequently, in newborns, Type 1 candidates of myodural bridge, that is, a thick connective tissue band from a common covering fascia of the Rma and Rmi, seemed to be much more evident than weak Type 2 candidates from the upper margin of the Rmi. However, force transmission via the Type 1 connective tissue band was likely to be limited or ineffective because of no or few connections between a muscle fiber and a composite collagen bundle in the covering fascia. A postnatal growth of the suboccipital fasciae and muscles might determine whether or not an "effective" bridge is established to induce a suggested headache. Individual variations in topographical relation among the prenatal occiput,

AX, and AT were likely to influence the morphology-symptom connection.

ACKNOWLEDGMENTS

We are grateful to families who donated their babies to the university and to Mr. Park, Jinkyu, the statistician, regional cardiocerebrovascular disease center for his help and valuable assistance in the statistical analysis of the data.

CONFLICT OF INTERESTS

The authors have no financial conflict of interests.

ETHICAL STANDARDS

The authors declare that all procedures contributing to this work complied with the ethical standards of the relevant national guidelines on human experimentation and with the Helsinki Declaration of 1995, as revised in 2000, and that the study was approved by the relevant institutional committees (no. 1428).

ABBREVIATIONS

AOM	posterior atlanto-occipital membrane
AT	atlas
AX	axis
OC	occipital bone
Oci	obliquus capitis inferior
MU	multifidus
Rma	rectus capitis posterior major
Rmi	rectus capitis posterior minori
SC	semispinalis capitis

REFERENCES

Abe H, Ishizawa A, Cho KH, Suzuki R, Fujimiya M, Rodríguez-Vázquez JF, Murakami G. 2012. Fetal development of the transverse Atlantis and alar ligaments at the craniovertebral junction. Clin Anat 25:714–721.

Abe S, Nakamura T, Rodriguez-Vazquez JF, Murakami G, Ide Y. 2011. Early fetal development of the rotator interval region of the shoulder with special reference to topographical relationships among related tendons and ligaments. Surg Radiol Anat 33:609–615.

Cho KH, Jang HS, Abe H, Yamamoto M, Murakami G, Shibata S. 2018a. Fetal development of fasciae around the arm and thigh muscles: A study using late stage fetuses. Anat Rec 301:1235–1243.

Cho KH, Jin ZW, Abe H, Shibata S, Murakami G, Rodríguez-Vázquez JF. 2016. Neural-dural transition at the thoracic and lumbar spinal nerve roots: A histological study of human late-stage fetuses. Biomed Res Int 2016:8163519.

Cho KH, Jin ZW, Abe H, Wilting J, Murakami G, Rodríguez-Vázquez JF. 2018b. Tensor fasciae latae muscle in human embryos and foetuses with special reference to its contribution to the development of the iliotibial tract. Folia Morphol 77:703–710.

Demer JL, Miller JM, Poukens V, Vinters HV, Glasgow BJ. 1995. Evidence for fibromuscular pulleys of the recti extraocular muscles. Investig Ophthalmol Vis Sci 36:1125–1136.

Eng CM, Arnold AS, Biewener AA, Lieberman DE. 2015. The human iliotibial band is specialized for elastic energy storage compared with the chimp fascia lata. J Exp Biol 218:2382–2393.

Gerlach U, Lierse W. 1990. Functional construction of the superficial and deep fascia system of the lower limb in man. Cells Tissues Organs 139:11–25.

Hayashi T, Kumasaka T, Mitani K, Yao T, Suda K, Seyama K. 2010. Loss of heterozygosity on tuberous sclerosis complex genes in multifocal micronodular pneumocyte hyperplasia. Mod Pathol 23: 1251.

Hinata N, Murakami G. 2014. The urethral rhabdosphincter, levator ani muscle, and perineal membrane: A review. Biomed Res Int 2014:1–18.

Huijing PA. 1999. Muscle as a collagen fiber reinforced composite: A review of force transmission in muscle and whole limb. J Biomech 32:329–345.

Jin Z, Jin Y, Yamamoto M, Abe H, Murakami G, Yan TF. 2016. Oblique cord (chorda obliqua) of the forearm and muscle-associated fibrous tissues at and around the elbow joint: A study of human foetal specimens. Folia Morphol 75:493–502.

Kahkeshani K, Ward PJ. 2012. Connection between the spinal dura mater and suboccipital musculature: Evidence for the myodural bridge and a route for its dissection—A review. Clin Anat 25:415–422.

Katori Y, Kawase T, Cho KH, Abe H, Rodríguez-Vázquez JF, Murakami G, Abe S. 2012. Prestyloid compartment of the parapharyngeal space: A histological study using late-stage human fetuses. Surg Radiol Anat 34:909–920.

Katori Y, Kawase T, Cho KH, Abe H, Rodríguez-Vázquez JF, Murakami G, Fujimiya M. 2013. Suprahyoid neck fascial configuration, especially in the posterior compartment of the parapharyngeal space: A histological study using late-stage human fetuses. Clin Anat 26:204–212.

Kim JH, Kinugasa Y, Yu HC, Murakami G, Abe S, Cho BH. 2015. Lack of striated muscle fibers in the longitudinal anal muscle of elderly Japanese: A histological study using cadaveric specimens. Int J Colorectal Dis 30:43–49.

Kinoshita H, Umezawa T, Omine Y, Kasahara M, Rodriguez-Vazquez JF, Murakami G, Abe S. 2013. Distribution of elastic fibers in the head and neck: A histological study using late-stage human fetuses. Anat Cell Biol 46:39–48.

Kinugasa Y, Arakawa T, Abe H, Abe S, Cho BH, Murakami G, Sugihara K. 2012. Anococcygeal raphe revisited: A histological study using mid-term human fetuses and elderly cadavers. Yonsei Med J 53:849–855.

Kinugasa Y, Niikura H, Murakami G, Suzuki D, Saito S, Tatsumi H, Ishii M. 2008. Development of the human hypogastric nerve sheath with special reference to the topohistology between the nerve sheath and other prevertebral fascial structures. Clin Anat 21:558–567.

Kono R, Poukens V, Demer JL. 2002. Quantitative analysis of the structure of the human extraocular muscle pulley system. Invest Ophthalmol Vis Sci 43:2923–2932.

Mackey AL, Heinemeier KM, Koskinen SOA, Kjaer M. 2008. Dynamic adaptation of tendon and muscle connective tissue to mechanical loading. Connect Tissue Res 49:165–168.

Motohashi O, Suzuki M, Shida N, Umezawa K, Ohtoh T, Sakurai Y, Yoshimoto T. 1995. Subarachnoid hemorrhage induced proliferation of leptomeningeal cells and deposition of extracellular matrices in the arachnoid granulations and subarachnoid space. Acta neurochirurgica 136:88–91.

Matsubara A, Murakami G, Niikura H, Kinugasa Y, Fujimiya M, Usui T. 2009. Development of the human retroperitoneal fasciae. Cells Tissues Organs 190:286–296.

Nash L, Nicholson H, Lee AS, Johnson GM, Zhang M. 2005. Configuration of the connective tissue in the posterior atlanto-occipital interspace: A sheet plastination and confocal microscopy study. Spine 30:1359–1366.

Osanai H, Murakami G, Ohtsuka A, Suzuki D, Nakagawa T, Tatsumi H. 2009. Histotopographical study of human periocular elastic fibers

using aldehyde-fuchsin staining with special reference to the sleeve and pulley system for extraocular rectus muscles. Anat Sci Int 84:129–140.
Pontell ME, Scali F, Enix DE, Battaglia PJ, Marshall E. 2013. Histological examination of the human obliquus capitis inferior myodural bridge. Ann Anat 195:522–526.
Range RL, Woodburne RT. 1964. The gross and microscopic anatomy of the transverse cervical ligament. Am J Obstet Gynecol 90:460–467.
Sakanaka K, Yamamoto M, Hirouchi H, Kim JH, Murakami G, Rodríguez-Vázquez JF, Abe SI. 2019. A joint disc-like structure at the median atlanto-axial joint in human fetuses. Anat Cell Biol submitted.
Sasaki H, Hinata N, Kurokawa K, Murakami G. 2014. Supportive tissues of the vagina with special reference to a fibrous skeleton in the perineum: A review. Open J Obstet Gynecol 4:144–157.
Scali F, Pontell ME, Nash LG, Enix DE. 2015. Investigation of meningomyovertebral structures within the upper cervical epidural space: A sheet plastination study with clinical implications. Spine J 15:2417–2424.
Shinomiya K, Dawson J, Spengler DM, Konrad P, Blumenkopf B. 1996. An analysis of the posterior epidural ligament role on the cervical spinal cord. Spine 21:2081–2088.
Shiraishi Y, Jin ZW, Mitomo K, Yamamoto M, Murakami G, Abe H, Wilting J, Abe S. 2018. Foetal development of the human gluteus maximus muscle with special reference to its fascial insertion. Folia Morphol 77:144–150.
Stopak D, Harris AK. 1982. Connective tissue morphogenesis by fibroblast traction. Dev Biol 90:383–398.
Trotter JA. 1993. Functional morphology of force transmission in skeletal muscle. A brief review. Acta Anat 146:205–222.
Venne G, Rasquinha BJ, Kunz M, Ellis RE. 2017. Rectus capitis posterior minor: Histological and biomechanical links to the spinal dura mater. Spine 42:E466–E473.
Yabuki Y. 2016. Clinical anatomy of the subserous layer: An amalhamation of gross and clinical anatomy. Clin Anat 29: 508–515.
Yuan X-Y, Yu S-B, Liu C, Xu Q, Zheng N, Zhang J-F, Chi Y-Y, Wang X-G, Lin X-T, Sui H-J. 2017. Correlation between chronic headaches and the rectus capitis posterior minor muscle: A comparative analysis of cross-sectional trail. Cephalalgia 37:1051–1056.
Zheng N, Chi YY, Yang XH, Wang NX, Li YL, Ge YY, Zhang LX, Liu TY, Yuan XY, Yu SB, Sui HJ. 2018. Orientation and property of fibers of the myodural bridge in humans. Spine J 18:1081–1087.
Zheng N, Yuan XY, Li YF, Chi YY, Gao HB, Zhao X, Yu SB, Sui HJ, Sharkey J. 2014. Definition of the to be named ligament and vertebrodural ligament and their possible effects on the circulation of CSF. PloS One 9:e103451.
Zumpano MP, Hartwell S, Jagos CS. 2006. Soft tissue connection between rectus capitus posterior minor and the posterior atlanto-occipital membrane: A cadaveric study. Clin Anat 19: 522–527.